Acta Pharmacologica Sinica

ARTICLE

GJA1-20k attenuates Ang II-induced pathological cardiac hypertrophy by regulating gap junction formation and mitochondrial function

Yi-le Fu[1], Liang Tao[1], Fu-hua Peng[1], Ning-ze Zheng[1], Qing Lin[1], Shao-yi Cai[1] and Qin Wang[1]

Cardiac hypertrophy (CH) is characterized by an increase in cardiomyocyte size, and is the most common cause of cardiac-related sudden death. A decrease in gap junction (GJ) coupling and mitochondrial dysfunction are important features of CH, but the mechanisms of decreased coupling and energy impairment are poorly understood. It has been reported that GJA1-20k has a strong tropism for mitochondria and is required for the trafficking of connexin 43 (Cx43) to cell–cell borders. In this study, we investigated the effects of GJA1-20k on Cx43 GJ coupling and mitochondrial function in the pathogenesis of CH. We performed hematoxylin–eosin (HE) and Masson staining, and observed significant CH in 18-week-old male spontaneously hypertensive rats (SHRs) compared to age-matched normotensive Wistar-Kyoto (WKY) rats. In cardiomyocytes from SHRs, the levels of Cx43 at the intercalated disc (ID) and the expression of GJA1-20k were significantly reduced, whereas JAK-STAT signaling was activated. Furthermore, the SHR rats displayed suppressed mitochondrial GJA1-20k and mitochondrial biogenesis. Administration of valsartan (10 mg· kg^{-1}· d^{-1}, i.g., for 8 weeks) prevented all of these changes. In neonatal rat cardiomyocytes (NRCMs), overexpression of GJA1-20k attenuated Ang II-induced cardiomyocyte hypertrophy and caused elevated levels of GJ coupling at the cell–cell borders. Pretreatment of NRCMs with the Jak2 inhibitor AG490 (10 μM) blocked Ang II-induced reduction in GJA1-20k expression and Cx43 gap junction formation; knockdown of Jak2 in NRCMs significantly lessened Ang II-induced cardiomyocyte hypertrophy and normalized GJA1-20k expression and Cx43 gap junction formation. Overexpression of GJA1-20k improved mitochondrial membrane potential and respiration and lowered ROS production in Ang II-induced cardiomyocyte hypertrophy. These results demonstrate the importance of GJA1-20k in regulating gap junction formation and mitochondrial function in Ang II-induced cardiomyocyte hypertrophy, thus providing a novel therapeutic strategy for patients with cardiomyocyte hypertrophy.

Keywords: cardiac hypertrophy; gap junctions; GJA1-20k; JAK-STAT; mitochondria; angiotensin II

Acta Pharmacologica Sinica (2021) 42:536–549; https://doi.org/10.1038/s41401-020-0459-6

INTRODUCTION

Cardiac hypertrophy (CH) is initially an adaptive process that is initiated by signaling cascades in response to injury, increased pressure overload or neurohormonal activation [1–4]. However, prolonged hypertrophy as a consequence of pathological stress leads to maladaptive changes that increase the risks of fatal ventricular arrhythmias [3]. CH is characterized by a thickened ventricular wall, an increase in cardiomyocyte size filled with excessive myofibril formation, enhanced protein synthesis, and the reactivation of several fetal genes (atrial natriuretic peptide [ANP], β-myosin heavy chain [β-MHC], etc.) [2, 5]. Among pro-hypertrophic factors, such as Ang II, catecholamines, thrombin, endothelin-1, lysophosphatidic acid, and transforming growth factor-β, Ang II is the most important factor for pressure overload-induced CH [2].

Gap junctions (GJs) are clusters of transmembrane channels that directly link the cytoplasmic compartments of neighboring cells to form conduits, enabling direct intercellular communication of chemical and electrical signals [6]. Cardiac pathologies are frequently associated with connexin redistribution, which is a form of gap junction remodeling [7, 8]. Decreased expression and distribution of Cx43 in cardiomyocytes has been described in patients with hypertrophic cardiomyopathies [9, 10], dilated cardiomyopathies [10, 11], ischemic cardiomyopathies [9, 10], clinical congestive heart failure [12], and hereditary disorders [13]. Decreased Cx43 expression and/or altered subcellular localization of Cx43 have been described in nearly every type of cardiac pathology [14]. Disruption of the side-to-side cell connections in hypertrophy caused by interstitial fibrosis, for instance, has been shown to impair cellular impulse propagation [15]. However, little is known about the exact mechanisms or signaling pathways regulating connexin trafficking and expression during hypertrophic remodeling.

On the other hand, the heart needs a persistent and steady supply of energy to constantly pump blood in and out and drive circulation [16]. Mitochondria make up approximately one-third of cardiomyocyte volume and supply approximately 90% of adenosine triphosphate (ATP). However, in the CH heart, the

[1]Department of Pharmacology, Zhongshan School of Medicine, Sun Yat-Sen University, Guangzhou 510080, China
Correspondence: Qin Wang (wangqin6@mail.sysu.edu.cn)
These authors contributed equally: Yi-le Fu, Liang Tao.

Received: 2 March 2020 Accepted: 7 June 2020
Published online: 3 July 2020

maximum rate of ATP hydrolysis and maximum contraction time of cardiac muscles are decreased, accompanied by deteriorated cardiac function [17]. Thus, the impairment of energy metabolism has been regarded as one of the main pathogenic mechanisms of CH [16].

In recent years, it has been reported that Cx43 can be involved in noncanonical events, such as cancer progression, muscle differentiation, and gene regulation and development [18–21]. Several decades of research on Cx43 has revealed that many of its functional roles are attributable to its C-terminal domain (CT) and not to the formation or existence of intercellular channels. It was recently found that GJA1 mRNA undergoes alternative translation to generate truncated N-terminal isoforms, of which GJA1-20k is the most abundant [22]. More importantly, GJA1-20k is required for the trafficking of connexin 43 (Cx43) to cell–cell borders [22], and it has a strong tropism for mitochondria [23]. In addition, GJA1-20k acts as an endogenous stress response protein that induces mitochondrial biogenesis and metabolic hibernation, preconditioning the heart against I/R insults [24]. In this report, we hypothesize that GJA1-20k may protect against CH by regulating gap junction formation and mitochondrial function. To verify our hypothesis, we carried out a series of in vitro and in vivo experiments to gain more insight into the potential effects of GJA1-20k on CH.

MATERIALS AND METHODS

Antibodies and reagents

Anti-Cx43 and anti-β-tubulin antibodies and HRP-conjugated secondary antibodies for use in Western blotting (WB) were purchased from Sigma-Aldrich (St. Louis, MO, USA). DMEM (high glucose) and Lipofectamine 3000 were purchased from Invitrogen (Carlsbad, CA, USA). TRIzol was obtained from Life Technologies (Carlsbad, CA, USA). cDNA Synthesis SuperMix kit and qPCR SuperMix were acquired from Transgen Biotech (Beijing, China). A BCA protein assay kit was obtained from Bio-Rad (Hercules, CA, USA). A chemiluminescent HRP substrate kit was purchased from Millipore Corporation (Billerica, MA, USA). Anti-cTnT, anti-Tom20, anti-vinculin, anti-mtCO2, anti-mtTFA, anti-PGC-1α, anti-RNF1, and anti-Mitofusin1 antibodies were purchased from Santa Cruz (Dallas, TX, USA). Anti-GAPDH antibody was obtained from Ray Antibody Biotech (Beijing, China). Anti-Jak2, anti-p-Jak2 (Tyr1007/1008), anti-Stat3, anti-p-Stat3 (Tyr705), anti-Cox IV, and anti-p-Drp1 (Ser616) primary antibodies were acquired from Cell Signaling Technology (Danvers, MA, USA).

Animal model and blood pressure (BP) measurement

All animal experimental procedures were performed in accordance with the policies of the Sun Yat-Sen University Animal Care and Use Committee and conformed to the Institutional Animal Care. Nine-week-old male SHRs ($n = 20$) and age-matched male Wistar-Kyoto (WKY) rats ($n = 10$) were purchased from Vital River Laboratories (Beijing, China). The SHRs were randomly separated into two groups: SHRs were administered 10 mg·kg^{-1}·d^{-1} valsartan (SHR-Val) intragastrically for 8 weeks. SHRs received vehicle (saline) treatment as a control (SHR). Age-matched WKY rats that received a vehicle (saline) for 8 weeks were also used as controls (WKY). Rat BP was measured before and after treatment with valsartan using a sphygmomanometer for rodents (BP2010A; Softron, Japan). Eight weeks after treatment, the rat hearts were harvested, weighed, and snap-frozen in liquid nitrogen.

Primary culture of neonatal rat cardiomyocytes (NRCMs)

The procedure for the isolation and culture of NRCMs was described previously [25]. Briefly, to isolate NRCMs, the rat ventricles were excised from 2-day-old Sprague Dawley rats, rinsed twice with ice-cold saline, and one-third of the heart was cut from the apex, minced into pieces smaller than 1 mm^3, and incubated overnight at 4 °C in D-Hanks balanced salt solution containing 0.1% trypsin. These small pieces were then collected and digested further with type-II collagenase (100 U/mL) at 37 °C for 10 min. The digestion supernatant was collected by adding an equal volume of DMEM supplemented with 10% FBS, and type-II collagenase buffer was added to continue digestion of the cardiac tissues at 37 °C for 10 min. The digestion was repeated 3–4 times until few remaining light-colored tissues remained, and a total of 3–4 tubes of cell suspension were collected. These cell suspensions were filtered through a cellular strainer and incubated in DMEM with 10% FBS for 2 h. Cells in the suspension were collected and plated at a density of 1×10^5–5×10^5 cells/mL and cultured in DMEM with 10% FBS, 100 U/mL penicillin, 100 μg/mL streptomycin, and 0.1 mM bromodeoxyuridine. The purity of the cardiomyocytes isolated using this method was >85% (Supplementary Fig. S1), according to flow cytometry (FCM) analysis.

Flow cytometry

Purity assessment was performed using FCM analysis, as described previously [26], with slight changes. Briefly, after 48 h of culture, the medium was removed, and the cells were washed twice with PBS and digested for 3–5 min with 0.25% trypsin at room temperature. Then, the digestion was stopped with DMEM with 10% FBS to prepare a suspension of individual cells by complete mixing. The cell suspension was centrifuged at 1000×*g* for 5 min, and the supernatants were discarded. After washing three times with PBS, the cell suspension was fixed in fixation buffer for 30 min and then permeabilized with permeabilization buffer for another 30 min. After washing three times with PBS, the cells were blocked in PBS with 5% donkey serum at room temperature for 1 h, followed by incubation at room temperature for 1 h with primary anti-cTnT antibody. After washing three times with PBS, the cells were incubated with the secondary antibody at room temperature for 1 h, and then the samples were analyzed by a Beckman CytoFLEX cytometer (Brea, CA, USA).

Western blotting

Cultured cells were washed with cold PBS and then harvested in cell lysis buffer. Whole cell lysates were sonicated and then centrifuged at 12,000×*g* for 30 min at 4 °C. The protein concentration was determined using a BCA protein assay kit. Fifteen micrograms of protein from the sample was separated by SDS–PAGE followed by transfer to a nitrocellulose membrane. The membranes were blocked with 5% (w/v) skim milk and were then incubated overnight with primary antibodies at 4 °C. After being washed three times with TBST, the membranes were incubated with HRP-conjugated secondary antibodies for 2 h at room temperature. The membranes were then washed with TBST before being visualized using a chemiluminescent HRP substrate kit immunoreactive solution and scanned using an ImageQuant LAS 4000. The expression values for each target protein were normalized to the corresponding expression values of vinculin, GAPDH, or β-tubulin.

Quantitative real-time polymerase chain reaction (qPCR)

The procedure for qPCR was the same as described previously [27]. After total RNA extraction using TRIzol, RNA concentrations were measured using a Nanodrop 2000 spectrophotometer (Thermo Fisher, Waltham, MA, USA). Reverse transcription to cDNA was performed using a cDNA Synthesis SuperMix kit on a C1000 Thermal Cycler instrument (Bio-Rad, CA, USA). Next, cDNA samples (2 μL) were used for qPCR with a qPCR SuperMix kit, and amplification was conducted for 40 cycles on a StepOnePlus Real-Time PCR system (Applied Biosystems, Foster, CA, USA). Rat-specific primers for β-MHC, ANP and GAPDH

(Supplementary Table S1) were synthesized by Sangon (Shanghai, China). GAPDH served as an endogenous control.

Tissue immunofluorescence

For tissue immunofluorescence, cryosections (10 μm) were fixed in 4% paraformaldehyde (PFA) and blocked in 5% normal donkey serum and 0.03% Triton X-100 in TBS. Each primary antibody was applied in 1% BSA and 0.03% Triton X-100 in TBS and incubated overnight at 4 °C. The following primary antibodies were used: anti-Cx43 (C6219, Sigma, 1:1000) and anti-cTnT (SC-20025, Santa Cruz, 1:200). The following day, the sections were incubated for 1 h at room temperature with the respective anti-mouse or anti-rabbit secondary antibody conjugated to Alexa Fluor (CST, 1:500), and then, the slides were mounted using ProLong gold with Hoechst 33258 (Sigma, 10 μg/mL). All images were acquired using an IX81 Olympus spinning disk confocal microscope.

Histological analysis

The procedure for the histological analysis was the same as previously described [28]. In brief, cardiac tissue was fixed in 10% neutral-buffered formalin for 24 h. The fixed hearts were embedded in paraffin and cut transversely into 4 μm sections. Heart sections were stained with hematoxylin and eosin (H&E). The cell surface area was determined with ImageJ 1.48v software (National Institutes of Health). The degree of collagen deposition was detected by Masson's trichrome staining. The percentage of fibrosis was calculated using a quantitative digital image analysis system (Image-Pro Plus 6.0). The fraction of the light blue-stained area normalized to the total area was used to indicate myocardial fibrosis. The cell images were captured with an Olympus IX81 spinning disk confocal microscope.

RNA interference

The siRNA transfection procedure was the same as previously described [27]. In brief, small inference RNA (siRNA) targeting Jak2 and the negative control (NC) were obtained from GenePharma (Shanghai, China). The sequences of the siRNAs are shown in Supplementary Table S2. Cardiomyocytes seeded in 35-mm dishes were transfected with 100 pmol of targeted siRNA or NC siRNA using 5 μL of Lipofectamine 3000 according to the manufacturer's instructions. Cardiomyocytes were transfected with siJak2 siRNA for 48 and 72 h for determination of mRNA and protein, respectively. The control groups were transfected with NC sequences.

Neonatal cardiomyocyte immunofluorescence

Ventricular cardiomyocytes from neonatal rats were fixed in 4% PFA for 30 min at room temperature, and then the cardiomyocytes were permeabilized and blocked with 0.03% Triton X-100 and 5% normal donkey serum in TBS for 1 h at room temperature. The cardiomyocytes were then incubated overnight with primary antibodies diluted in 1% BSA and 0.03% Triton X-100 in TBS at 4 °C. The primary antibodies used were rabbit anti-Cx43 (C6219, Sigma, 1:1000) and mouse anti-cTnT (SC-20025, Santa Cruz, 1:200). The cardiomyocytes were then incubated for 1 h at room temperature with diluted Alexa Fluor secondary antibodies (1:500, CST). The cardiomyocyte coverslips were then mounted with ProLong gold with Hoechst 33258 (Sigma) for image acquisition using an IX81 Olympus spinning disk confocal microscope.

Gene set enrichment analysis (GSEA)

Gene expression data sets with series number GSE89714 based on platform GPL11154 were downloaded from the Gene Expression Omnibus (GEO) database (http://www.ncbi.nlm.nih.gov/geo/). The data contained five hypertrophic hearts and four healthy hearts. RNA-Seq experiments were performed using Illumina HiSeq 2000 (Illumina, San Diego, CA, USA). Kyoto Encyclopedia of Genes and Genomes (KEGG) is a database for the systematic analysis of gene function that links genomic information with higher-level systemic functions [29]. GSEA [30] was performed to identify the pathways enriched with genes that were differentially expressed in the hypertrophic cardiomyopathic hearts and normal hearts; the cutoff values were $P < 0.05$ and FDR < 0.25.

Assessment of mitochondrial membrane potential

The mitochondrial membrane potential was measured with a commercial JC-1 kit (1 μM, Biosciences, St. Louis, MO, USA) following the manufacturer's instructions. Briefly, 24 h after GJA1-20k cDNA or an empty vector was transfected into cardiomyocytes, the cardiomyocytes were treated with Ang II (1 μM) for 48 h. These cells were rinsed with PBS and incubated in 1 mL of JC-1 staining solution at 37 °C for 30 min. JC-1 molecules enter the cytosol as monomers, emitting green fluorescence (535 nm), and when entering mitochondria, they form dimers/aggregates, emitting red fluorescence (570 nm). The intensity of red (aggregate JC-1)/green (monomeric JC-1) fluorescence was detected with an Olympus IX81 spinning disk confocal microscope. Red and green fluorescence intensity in the individual cardiomyocytes was quantified using ImageJ (NIH). The red-to-green fluorescence intensity ratio indicates the mitochondrial membrane potential.

Measurement of superoxide formation

After treatment, the cardiomyocytes were treated with MitoSOX red (5 μM, Thermo Fisher Scientific, USA) in HEPES buffer and incubated at 37 °C for 30 min. MitoSOX Red specifically targets mitochondria in live cells. The more superoxide that is produced in mitochondria, the greater the fluorescence intensity that is observed. After 30 min of incubation, the cells were washed two times with HEPES buffer. Live cell imaging of the cardiomyocytes was performed using an Olympus IX81 spinning disk confocal microscope. Red fluorescence intensity in an individual cardiomyocyte was quantified using ImageJ software (NIH), which indicated the mitochondrial superoxide production level.

Mitochondrial respiration assessment

NRCMs were plated (~10,000 cells/well) in an XF96-well plate (Seahorse Bioscience, Massachusetts, USA) and transfected with GJA1-20k or empty vector cDNA. Twenty-four hours later, the cells were treated with vehicle or Ang II (1 μM) for 48 h. The cells medium was then switched to XF base medium supplemented with 10 mM glucose, 10 mM pyruvate, and 4 mM L-glutamine and incubated in 0% CO_2 for 1 h before the test. The mitochondrial respiration oxygen consumption rate (OCR) was measured by a Seahorse Extracellular Flux Analyzer XF96 (Seahorse Bioscience) according to the manufacturer's instructions. First, basal respiration was measured in an unbuffered medium. Then, oligomycin (1 μM) was added to inhibit ATP synthesis and to detect the respiration linked to ATP production. The uncoupler carbonyl cyanide 4-(trifluoromethoxy) phenylhydrazone (FCCP, 1 μM) was applied to measure respiratory reserve capacity and maximal respiration. Finally, a combination of rotenone plus antimycin A (rot & AA, 0.5 μM) was added to inhibit complexes III and I, to completely block mitochondrial oxygen consumption.

Statistical analysis

The experimental data are expressed as the means ± SEM. Statistical analysis between two groups was performed by Student's *t*-test. For multiple comparisons, one-way analysis of variance (ANOVA) was used with Tukey's post hoc test. The analysis was performed using GraphPad Prism 7.0 (GraphPad Inc., La Jolla, CA, USA). In all cases, differences were considered significant at $P < 0.05$.

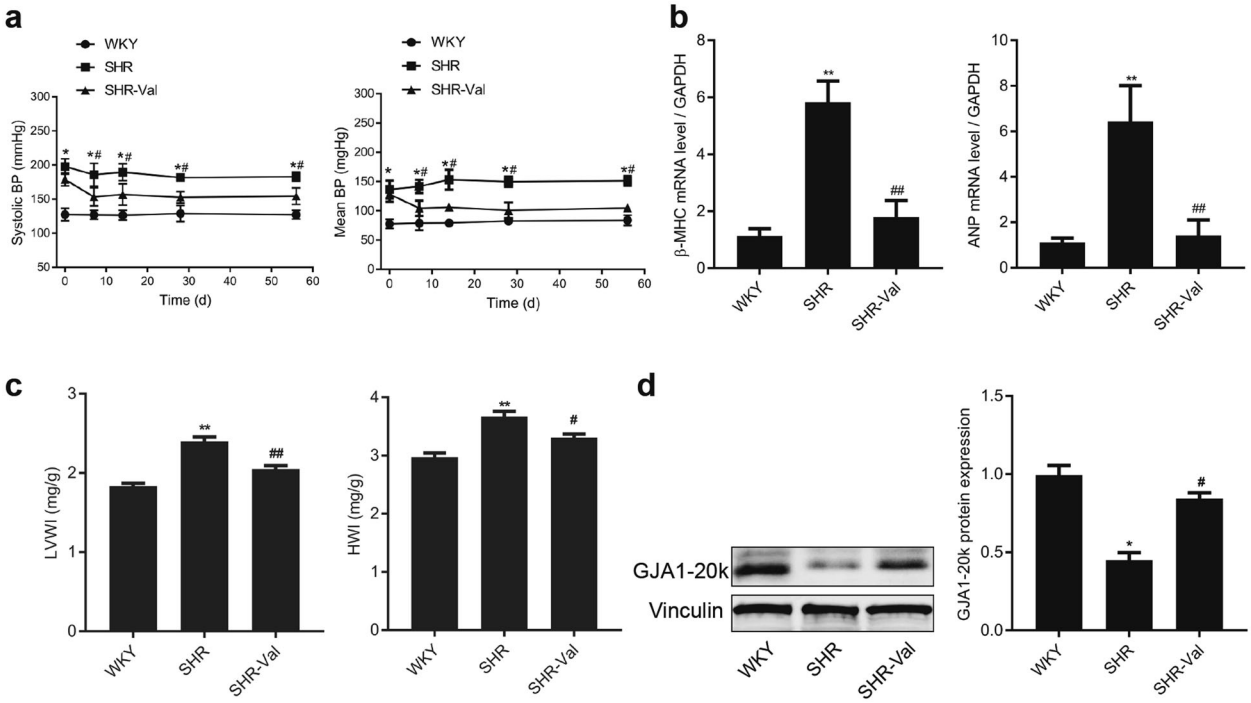

Fig. 1 GJA1-20k is downregulated in the spontaneously hypertensive rat (SHR) cardiac hypertrophy (CH) model. a The systolic (left) and mean (right) blood pressure (BP) of the Wistar-Kyoto (WKY) rats and SHRs were measured. WKY or SHR indicates the group of WKY rats or SHRs treated with saline; SHR-Val indicates the group of SHRs treated with valsartan (10 mg·kg^{-1}· d^{-1}). $n = 9$-10. $^{*}P < 0.05$ vs. WKY; $^{\#}P < 0.05$ vs. SHR. **b** The β-myosin heavy chain (β-MHC) and atrial natriuretic peptide (ANP) mRNA levels in rat myocardium as measured by real-time quantitative polymerase chain reaction (RT-qPCR). $n = 5$-6. $^{**}P < 0.01$ vs. WKY; $^{\#\#}P < 0.01$ vs. SHR. **c** The left ventricular weight index (LVWI) and the heart weight index (HWI). $n = 5$–6, $^{**}P < 0.01$ vs. WKY; $^{\#}P < 0.05$, $^{\#\#}P < 0.01$ vs. SHR. **d** Western blot results from heart tissue analysis. The blots are probed with an antibody for the Cx43 C-terminus and with an anti-vinculin antibody (left). Expression of GJA1-20k protein normalized to vinculin expression (right). $n = 5$–6. $^{*}P < 0.05$ vs. WKY. $^{\#}P < 0.05$ vs. SHR. Data are expressed as the means ± SEM.

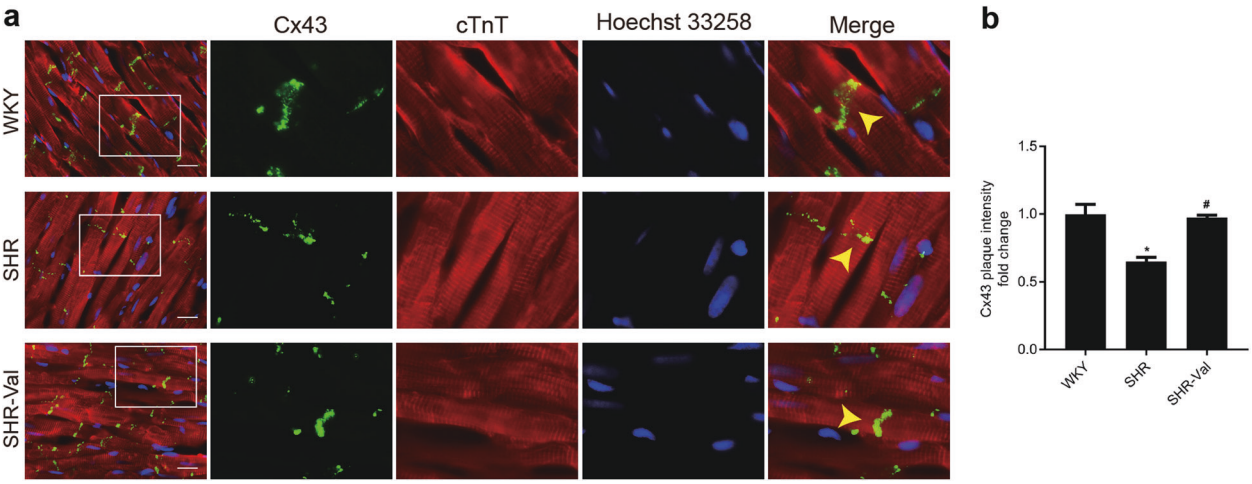

Fig. 2 Connexin 43 (Cx43) gap junction coupling at intercalated disks (IDs) is reduced in hypertrophic cardiomyocyte tissue. a Immunofluorescence staining of Cx43 (green) and cTnT (red, marking cardiomyocytes) in heart sections from different treatment groups (bar = 20 μm). Wistar-Kyoto (WKY) rats and spontaneously hypertensive rats (SHRs) indicate the group of WKY rats and SHRs treated with saline, respectively; SHR-Val indicates the group of SHRs treated with valsartan (10 mg· kg^{-1}· d^{-1}). Nuclei were counterstained with Hoechst 33258 (blue). **b** Quantification of Cx43 fluorescence intensity at ID regions ($n = 3$ hearts per group). Arrow: gap junction plaque at an ID. $n = 3$. $^{*}P < 0.05$ vs. WKY. $^{\#}P < 0.05$ vs. SHR. Data are presented as the means ± SEM.

RESULTS

Levels of Cx43 at intercalated discs and GJA1-20k expression are reduced in hypertrophic cardiomyocytes from the SHRs, and valsartan attenuates these changes

To elucidate the role of GJA1-20k in the pathogenesis of CH, spontaneously hypertensive rats (SHRs) and age-matched Wistar Kyoto (WKY) rats were used in the present study. Compared with the WKY rats, the SHRs treated with normal saline developed significant increases in both systolic and mean blood pressure (Fig. 1a) and significant increases in heart rates (Supplementary Fig. S2). Moreover, the expression of the hypertrophic markers β-MHC and ANP was also increased (Fig. 1b). CH was observed in the

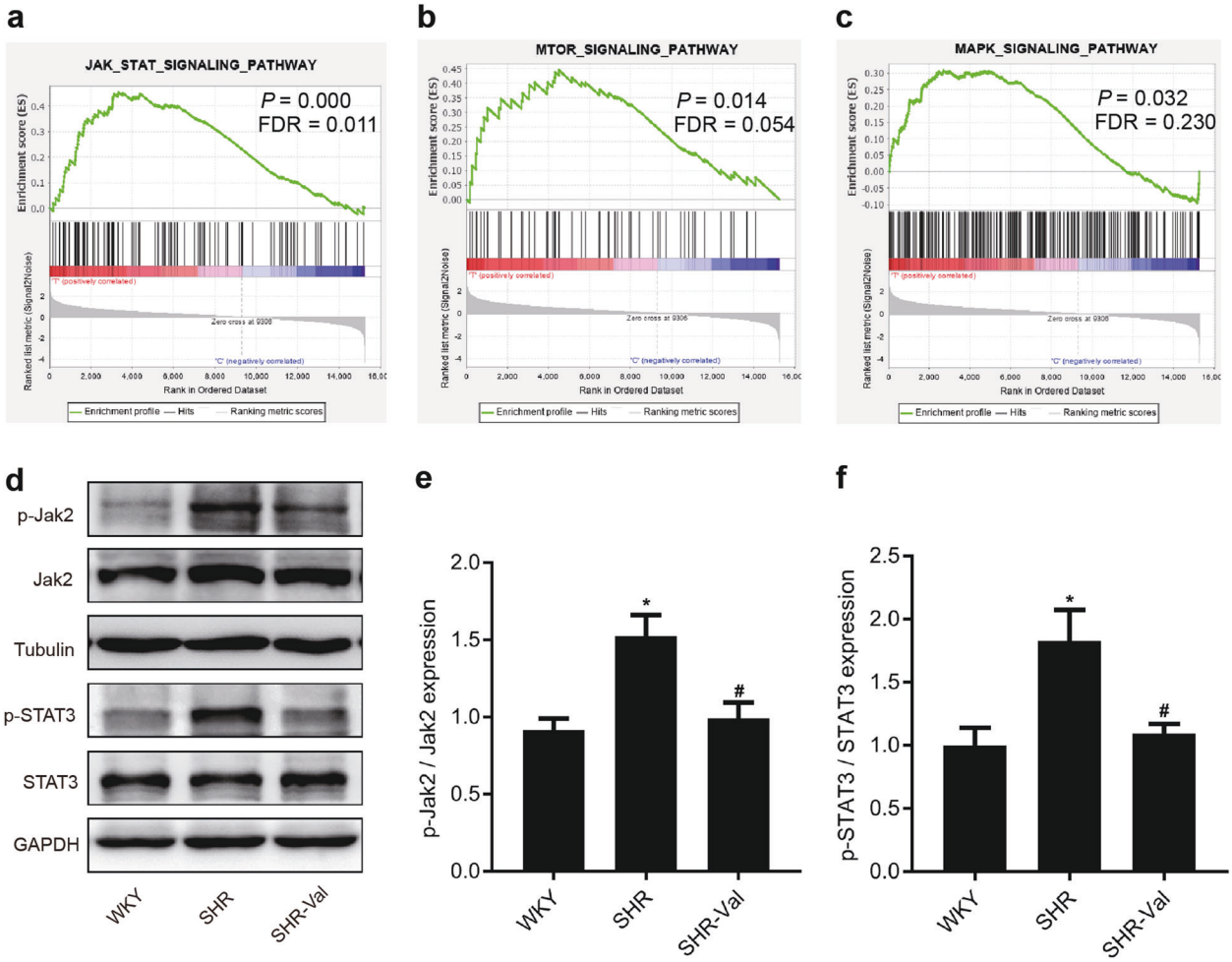

Fig. 3 The JAK-STAT pathway is activated in SHRs, and valsartan reduces this activation. a–c Gene set enrichment analysis (GSEA) of a hypertrophic cardiomyopathy heart gene expression profile data set (GSE89714) is shown, confirming the enrichment of the JAK-STAT, PI3K-AKT-mTOR, and MAPK-signaling pathways in hypertrophic cardiomyopathy. FDR false discovery rate. **d–f** Representative Western blot and quantitative results showing the expression levels of phosphorylated Jak2 and Stat3 and the total protein expression levels of Jak2 and Stat3 from the hearts of WKY rats, SHRs, and SHR-Val. Wistar-Kyoto (WKY) rats and spontaneously hypertensive rats (SHRs) indicate the group of WKY rats and SHRs treated with saline, respectively; SHR-Val indicates the group of SHRs treated with valsartan (10 mg· kg^{-1}· d^{-1}). $n = 5–6$. $^{*}P < 0.05$ vs. WKY; $^{\#}P < 0.05$ vs. SHR. Jak2 indicates Janus kinase 2; Stat3 indicates signal transducer and activator of transcription 3.

SHRs and was characterized by an elevation of myocytes in a cross-sectional area (Supplementary Fig. S3a,b) and by an increase in the left ventricular weight to heart weight index (LVWI) and heart weight to body weight index (HWI) (Fig. 1c). Assessment of myocardial fibrosis revealed that the SHRs developed interstitial and perivascular fibrosis (Supplementary Fig. S4a, b). A significant decrease in GJA1-20k protein levels in the ventricles of the SHRs was detected (Fig. 1d). Notably, two protein bands were attributed to GJA1-20k. We believe that one of the two protein bands was the phosphorylated form of GJA1-20k. Ul-Hussain and his colleagues reported that one to three bands are usually detected with antibodies directed against the carboxyl-terminal domain of GJA1-20k. A reduced density of GJs at IDs was observed in the hypertrophic cardiomyocytes from the SHRs (Fig. 2a, b). These data suggest that the downregulation of GJA1-20k expression may play a role in CH formation by restoring GJs.

To further explore the link between CH and GJA1-20k downregulation, we treated SHRs with valsartan (SHR-Val), which is an AT1R blocker. As expected, intragastric administration of valsartan significantly reduced blood pressure (Fig. 1a) and heart rate (Supplementary Fig. S2); suppressed the expression of two CH markers, β-MHC and ANP (Fig. 1b); reduced cell size (Supplementary Fig. S3a, b); attenuated interstitial and perivascular fibrosis (Supplementary Fig. S4a, b); and reduced the left ventricular weight index and heart weight index (Fig. 1c). Valsartan significantly upregulated GJA1-20k expression at the protein level (Fig. 1d) and clearly increased the GJs at IDs (Fig. 2a, b). These results suggest that the downregulation of GJA1-20k in the SHRs was induced by the activation of AT1R.

The JAK-STAT pathway is activated in the SHRs, and valsartan reduces this activation

The binding of Ang II to its receptor, AT1R, has been demonstrated to induce intracellular signal transduction that results in pathologic cardiac remodeling; this signaling involves mitogen-activated protein kinases (MAPKs), phosphatidylinositol 3-kinase (PI3K), protein kinase B (AKT), Janus-activating kinases (JAKs) and signal transducer, and activator of transcription (STAT) proteins [31]. We used a gene expression profile data set (GSE89714) based on the heart of a hypertrophic cardiomyopathy patient to confirm the enrichment of three signaling pathways (Fig. 3a–c and Supplementary Table S3). These results established a correlation between CH and three signaling pathways. The JAK-STAT-signaling pathway was the most significantly

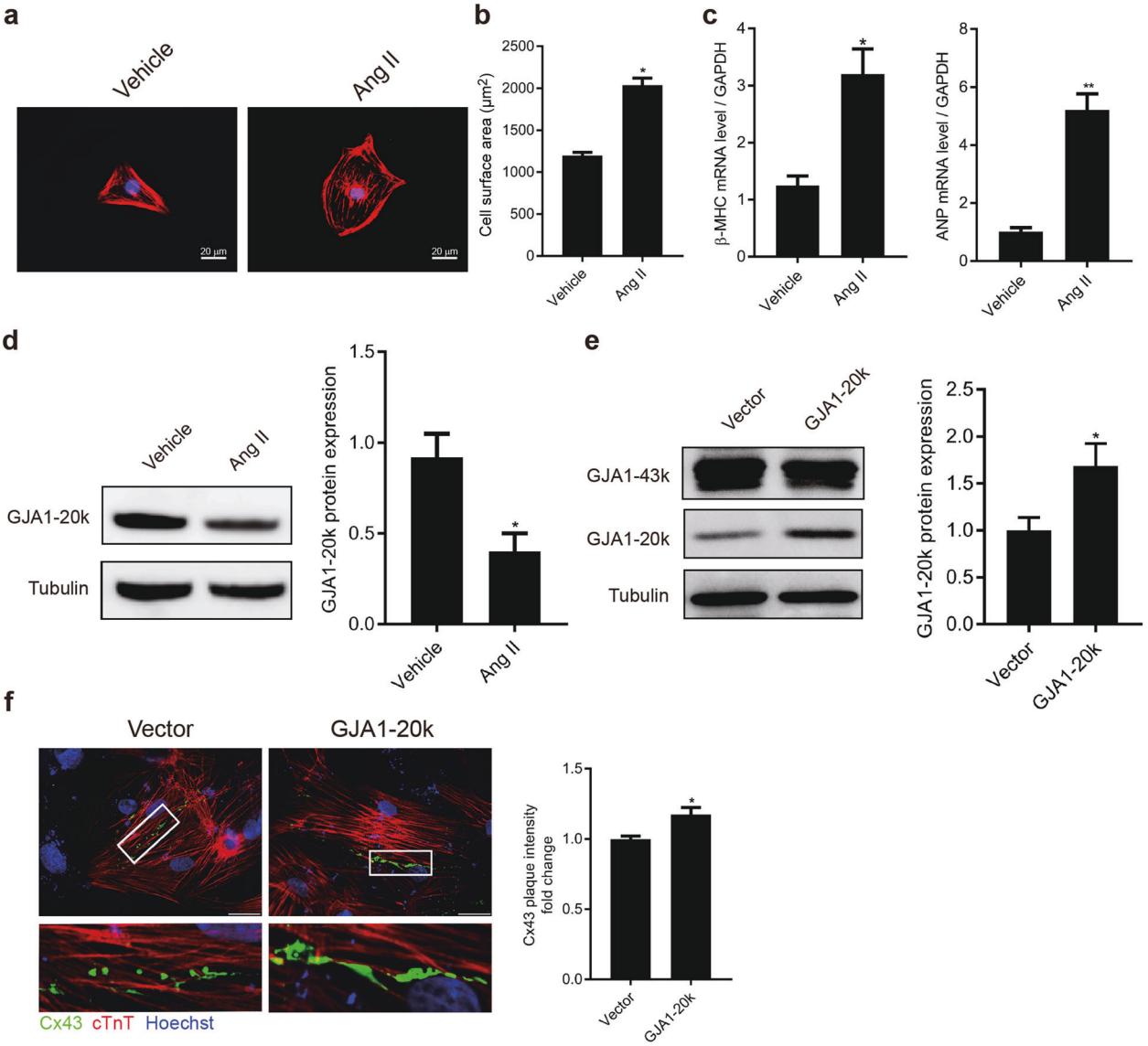

Fig. 4 Angiotensin II (Ang II) treatment induces cardiomyocyte hypertrophy (CH) and suppresses GJA1-20k expression. Neonatal rat cardiomyocytes (NRCMs) were treated with 1 μM Ang II for 48 h to induce CH. **a** Immunofluorescence of cardiomyocytes treated with or without Ang II (bar = 20 μm). **b** Quantification of cell surface areas (μm^2) in each group is shown for three independent experiments with >50 cells evaluated in each experiment. $n = 3$. $^*P < 0.05$ vs. vehicle (DMSO). **c** The β-myosin heavy **c**hain (β-MHC) and atrial natriuretic peptide (ANP) mRNA levels were measured by RT-qPCR. $n = 3$. $^*P < 0.05$, $^{**}P < 0.01$ vs. vehicle. **d** Western blot of cell lysates probed with GJA1-20k C-terminal antibody to determine the internally translated GJA1-20k (left). Quantification of GJA1-20k isoform levels (right). $n = 3$. $^*P < 0.05$ vs. vehicle. **e** Western blot analysis of NRCMs transfected with cDNA **e**ncoding GJA1-20k or transfected with an empty vector (left). Quantification of GJA1-20k levels (right). $n = 3$. $^*P < 0.05$ vs. vector. **f** Immunofluorescence of NRCMs transfected with the empty vector or GJA1-20k (left, bar = 20 μm). Quantification of connexin 43 (Cx43) fluorescence intensity at cell–cell borders in each group is shown for three independent experiments with >50 cells evaluated in each experiment (right). $n = 3$. $^*P < 0.05$ vs. vector. Cx43 (green) staining was performed to identify gap junction formation; cTnT staining (red) was performed to identify cardiomyocytes. Nuclei were counterstained with Hoechst 33258 (blue). $n = 3$. Data are presented as the means ± SEM.

associated with CH; therefore, we wondered whether GJA1-20k expression is regulated by the JAK-STAT-signaling pathways associated with translation. To assess the change in the JAK-STAT-signaling pathway, we used WB to determine the total and phosphorylated levels of Jak2 and Stat3 in the hypertrophic hearts of the SHRs. A significant increase in p-Jak2 was observed in the SHRs compared to that in the WKY rats (Fig. 3d–f), and a similar elevation in p-Stat3 was also observed. On the other hand, both p-Jak2 and p-Stat3 levels were significantly downregulated in the SHR-Val animals. Taken together, these data suggest that GJA1-20k may be regulated by JAK-STAT signaling during the development of CH.

GJA1-20k is suppressed during Ang II-induced NRCM hypertrophy

To further study whether GJA1-20k attenuates CH through JAK-STAT signaling, we used an in vitro model of cardiomyocyte hypertrophy in which hypertrophy is induced in NRCMs by Ang II (1 μM Ang II treatment for 48 h). Ang II-induced cardiomyocyte hypertrophy models were successfully established (Fig. 4a), as indicated by the elevation of cardiomyocyte size and increased expression of β-MHC and ANP (Fig. 4b, c). Then, the effects of Ang II on GJA1-20k in the NRCMs were explored. GJA1-20k expression was measured by WB (Fig. 4d) and was found to be significantly decreased in CH cells compared to the controls, which were treated only with vehicle.

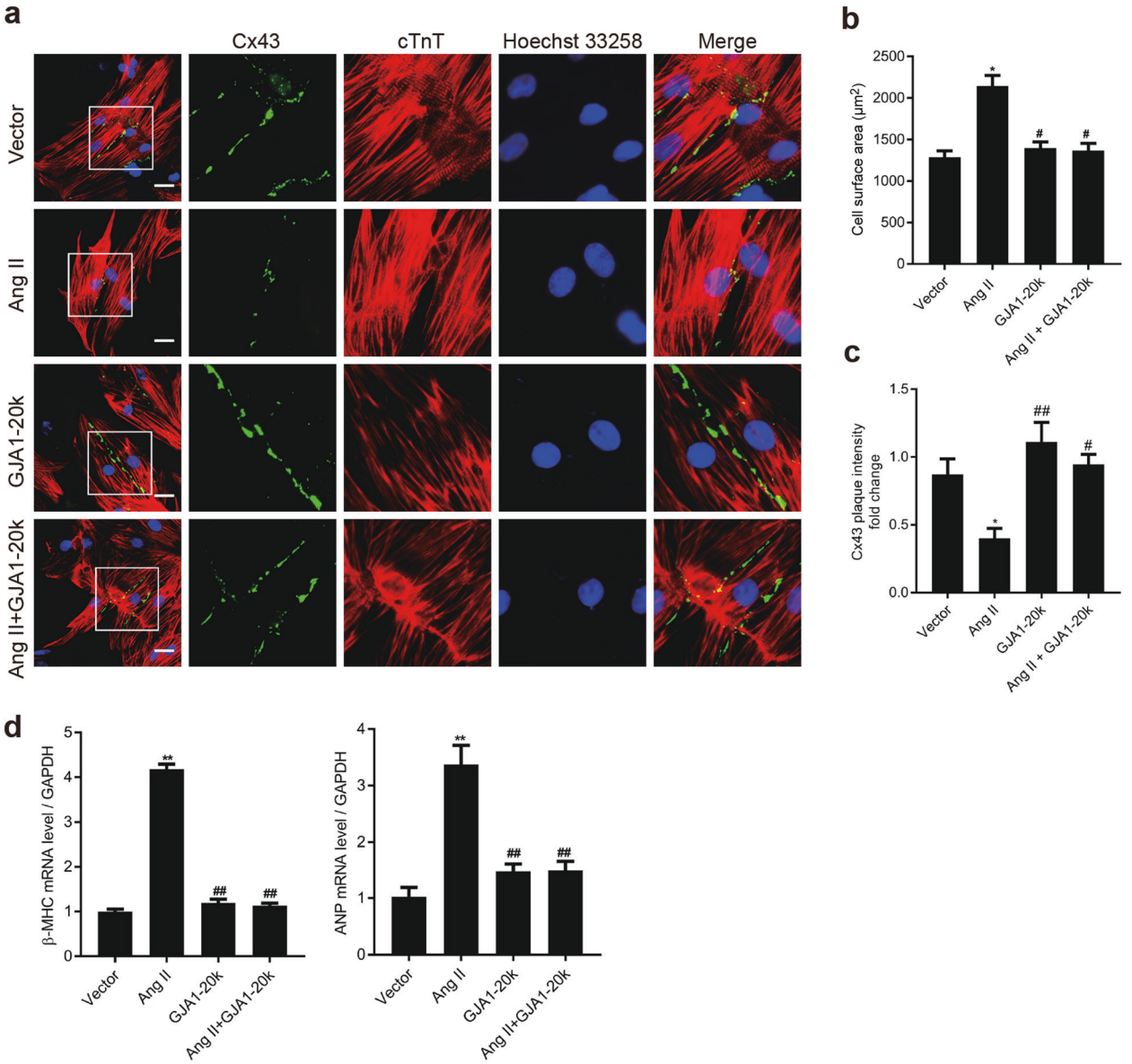

Fig. 5 GJA1-20k attenuates angiotensin II (Ang II)-induced cardiomyocyte hypertrophy (CH) by promoting gap junction formation in neonatal rat cardiomyocytes (NRCMs). NRCMs were transfected with an empty control vector or a construct carrying GJA1-20k cDNA for 24 h and then treated with vehicle (DMSO) or Ang II (1 μM) for 48 h. **a** Immunofluorescence detection of Cx43 gap junctions (green); cTnT staining (red) was performed to identify cardiomyocytes (Bar = 20 μm). Nuclei were counterstained with Hoechst 33258 (blue). **b** Quantification of the cell surface area (μm^2) of 50 NRCMs in each group is shown. $n = 3$. $^{*}P < 0.05$ vs. vector. $^{\#}P < 0.05$ vs. Ang II. **c** Quantification of Cx43 fluorescence intensity at cell–cell borders. $^{*}P < 0.05$ vs. vector. $^{\#}P < 0.05$, $^{\#\#}P < 0.01$ vs. Ang II. $n = 3$. **d** The β-myosin heavy chain (β-MHC) and atrial natriuretic peptide (ANP) mRNA levels were measured by RT-qPCR. $^{**}P < 0.01$ vs. vector. $^{\#\#}P < 0.01$ vs. Ang II. $n = 3$. Data are presented as the means ± SEM.

GJA1-20k regulates the trafficking of GJA1-43k molecules to cell–cell borders

Recently, Smyth and Shaw [22] provided evidence that GJA1-20k, the product of alternative translation of the GJA1 transcript, regulated the trafficking of GJA1-43k molecules to cell–cell borders. Therefore, we designed experiments to examine whether GJA1-20k had a similar function in NRCMs. As expected, transfection of cDNA containing the GJA1-20k-coding sequence under transcriptional regulation of the cytomegalovirus (CMV) promoter was sufficient to facilitate the expression of GJA1-20k but not GJA1-43k (Fig. 4e). Immunofluorescence of the NRCMs transfected with GJA1-20k cDNA revealed that gap junction plaques at cell–cell borders were significantly elevated compared to those observed in cells transfected with empty vector (Fig. 4f). These data indicate that GJA1-20k acted as a chaperone auxiliary protein, regulating the trafficking of GJA1-43k molecules to cell–cell borders, a finding consistent with the data from Smyth and Shaw.

GJA1-20k alleviates Ang II-induced NRCM hypertrophy by facilitating the trafficking of GJA1-43k to cell–cell borders

The results shown in Fig. 1 indicate that Ang II downregulated GJA1-20k expression. To assess the role of GJA1-20k in Ang II-induced CH, we analyzed the Ang II-induced cellular hypertrophic phenotype of the NRCMs by transfecting the cells with an empty vector or a vector carrying GJA1-20k cDNA. Compared to the cardiomyocytes transfected with the NC vector, the cardiomyocytes transfected with the GJA1-20k cDNA vector displayed a significant increase in Cx43 gap junction coupling at cell–cell borders, as well as an decreased cell size 48 h after Ang II

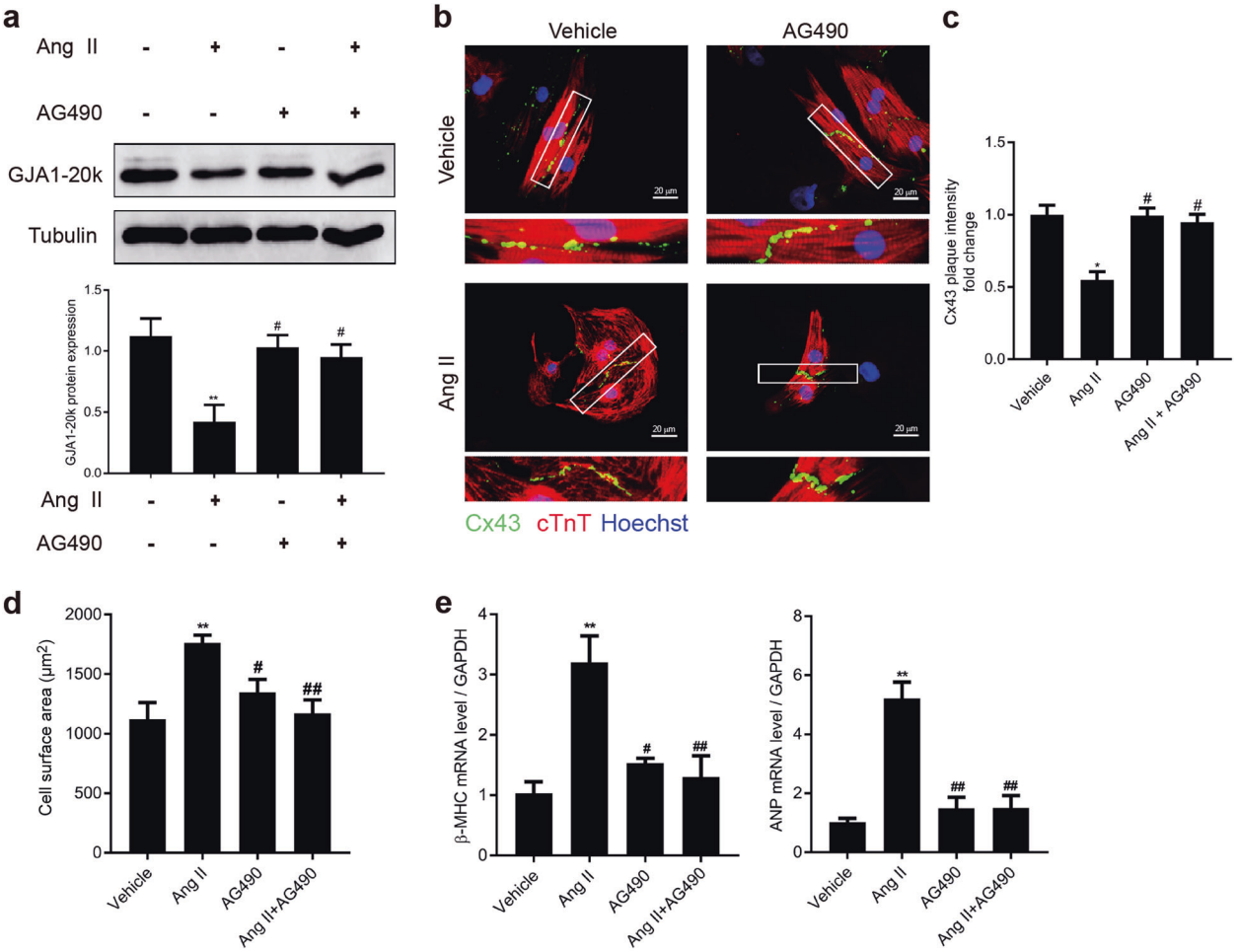

Fig. 6 AG490 attenuates angiotensin II (Ang II)-induced GJA1-20k downregulation and cardiomyocyte hypertrophy (CH). Neonatal rat cardiomyocytes (NRCMs) were treated with vehicle (DMSO) or 10 μM AG490 for 6 h, followed by the addition of Ang II (1 μM) for 48 h. **a** Western blot of cell lysates probed with connexin 43 (Cx43) C-terminal antibody to detect GJA1-20k (upper). Quantification of GJA1-20k band intensity (lower). $n = 3$. $^{**}P < 0.01$ vs. Ang II(−)/AG490(−); $^{\#}P < 0.05$ vs. Ang II(+)/AG490(−). **b** Immunofluorescence detection of Cx43 gap junctions (green); cTnT staining (red) was performed to identify cardiomyocytes. Nuclei were counterstained with Hoechst 33258 (blue). (Bar = 20 μm). **c** Quantification of Cx43 fluorescence intensity at cell–cell borders. $n = 3$. $^{*}P < 0.05$ vs. vehicle; $^{\#}P < 0.05$ vs. Ang II. **d** Quantification of the cell surface area (μm²) of 50 NRCMs in each group is shown. $n = 3$. $^{**}P < 0.01$ vs. vehicle; $^{\#}P < 0.05$, $^{\#\#}P < 0.01$ vs. Ang II. **e** The β-myosin heavy chain (β-MHC) and atrial natriuretic peptide (ANP) mRNA levels were measured by RT-qPCR. $n = 3$. $^{**}P < 0.01$ vs. vehicle; $^{\#}P < 0.05$, $^{\#\#}P < 0.01$ vs. Ang II. AG490 = Jak2 inhibitor. Data are presented as the means ± SEM.

treatment (Fig. 5a–c). β-MHC and ANP transcription were upregulated under the same treatment conditions (Fig. 5d). Impressively, in the cells transfected with GJA1-20k, we found that Cx43 formed GJs at cell–cell borders with unchanged mRNA levels of β-MHC or ANP and was accompanied by unchanged cell sizes 48 h after Ang II stimulation, suggesting that the cellular hypertrophy induced by Ang II was decreased in the presence of GJA1-20k expression. These results indicate that GJA1-20k plays a crucial role in Ang II-induced CH.

Inhibition of JAK-STAT signaling attenuates the Ang II-induced GJA1-20k decrease and cardiomyocyte hypertrophy

As shown in Fig. 3, p-Jak2 expression was increased in the myocardium of the SHRs. To test whether the downregulation of GJA1-20k and cell hypertrophy induced by Ang II in the NRCMs occurred through JAK-STAT signaling, we pretreated NRCMs with AG490, a Jak2 inhibitor, before adding Ang II. AG490 (10 μM) treatment significantly increased the Ang II-induced downregulation of the expression of GJA1-20k and restored the formation of GJs at the cell–cell borders (Fig. 6a–c). Moreover, the cell size was decreased (Fig. 6d). The transcription of β-MHC and ANP (Fig. 6e) was also decreased in a similar manner, suggesting that AG490 treatment could attenuate Ang II-induced hypertrophy. These data indicate that Jak2-mediated downregulation of GJA1-20k plays a key role in Ang II-induced cardiomyocyte hypertrophy.

Jak2 is the major kinase critical for Ang II-induced GJA1-20k downregulation and cardiomyocyte hypertrophy

To further validate our findings that GJA1-20k is regulated by Jak2, the effects of Jak2 on GJA1-20k expression and Ang II-induced cardiomyocyte hypertrophy were determined by reducing the expression of Jak2 by Jak2-specific siRNAs. The expression of Jak2 was stably reduced with siRNAs to 68% 48–72 h posttransfection (Fig. 7a). NRCMs in which Jak2 was knocked down were stimulated with Ang II (1 μM) for 48 h after transfection. The expression of GJA1-20k, GJs composed of Cx43 at the cell–cell borders, cell size, and CH markers were all measured. Knocking down Jak2 significantly promoted GJA1-20k expression and the formation of GJs composed of Cx43 (Fig. 7b–d). The inhibition of Jak2 also decreased cell size (Fig. 7e) and attenuated the expression of β-MHC and ANP (Fig. 7f, g) in the presence of Ang II. In summary, the present results indicated that Jak2 was the key contributor to

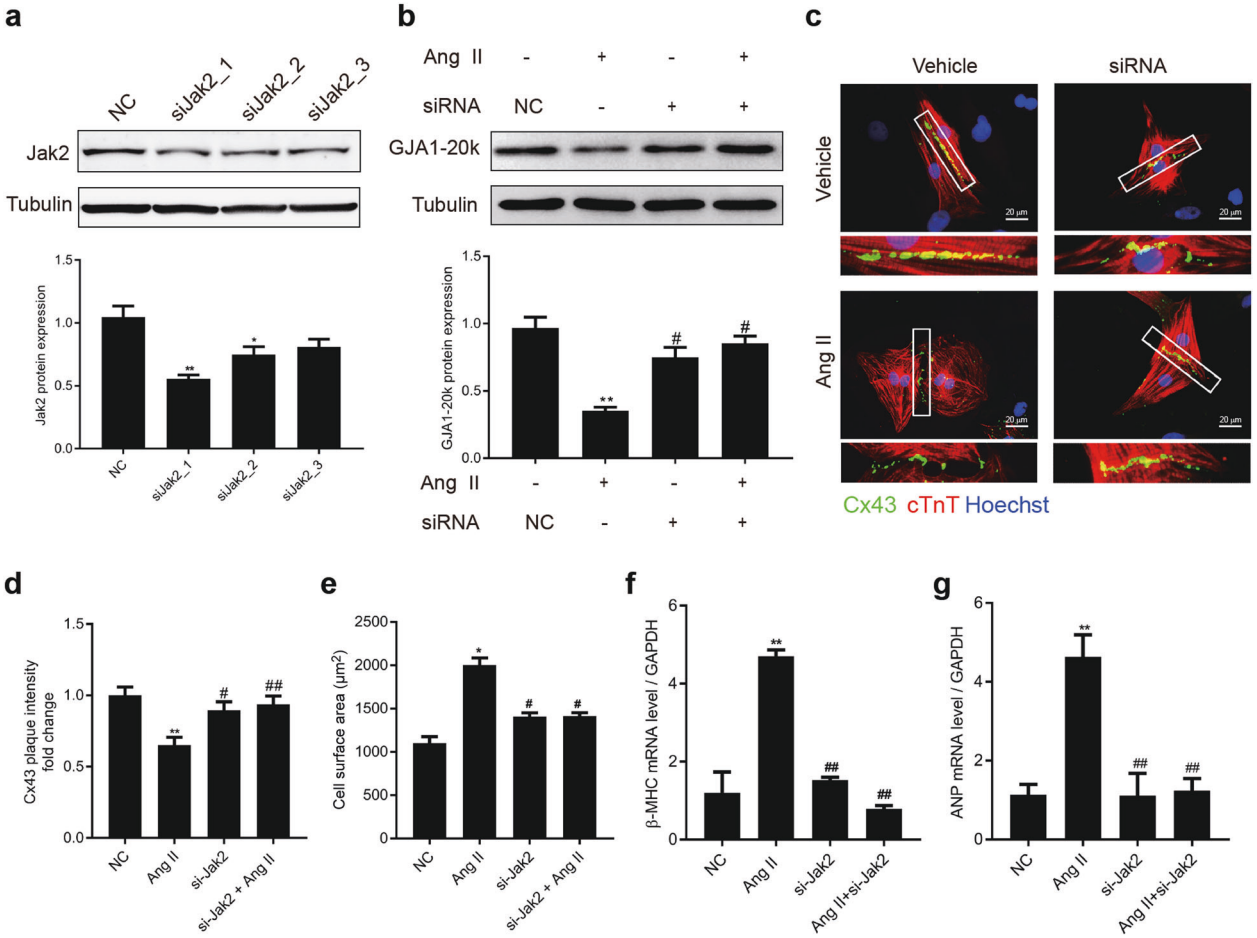

Fig. 7 Jak2 is the major kinase critical for angiotensin II (Ang II)-induced GJA1-20k downregulation and cardiomyocyte hypertrophy (CH). Neonatal rat cardiomyocytes (NRCMs) were transfected with siRNA against endogenous Jak2. **a** Whole cell extracts were resolved by Western blotting and immunoblotted with antibodies against Jak2 to confirm the knockdown of endogenous Jak2 (upper). Quantification of Jak2 band intensity (lower). $n = 3$. $^{*}P < 0.05$, $^{**}P < 0.01$ vs. negative control (NC). **b** NRCMs with endogenous Jak2 or a NC generated by knockdown were stimulated with Ang II (1 μM) for 48 h. GJA1-20k protein levels were measured by Western blotting using extracts from each condition as indicated (upper). The results are shown in a bar graph (lower). $n = 3$. $^{**}P < 0.01$ vs. siRNA(NC)/Ang II(−); $^{\#}P < 0.05$ vs. siRNA(−)/Ang II(+). **c** Representative images of NRCMs transfected with the indicated siRNA and then treated with vehicle (DMSO) or Ang II for 48 h (bar = 20 μm). Connexin 43 (Cx43) staining (green) was performed to identify gap junction formation. cTnT staining (red) was performed to determine cell size. **d** Quantification of Cx43 fluorescence intensity at cell–cell borders. $n = 3$. $^{**}P < 0.01$ vs. NC; $^{\#}P < 0.05$, $^{\#\#}P < 0.01$ vs. Ang II. **e** Quantification of the cell surface area (μm^2). At least 50 cells were quantified for each treatment. $n = 3$. $^{*}P < 0.05$ vs. NC; $^{\#}P < 0.05$ vs. Ang II. **f–g** RNA was subjected to RT-qPCR experiments to determine the mRNA levels of β-myosin heavy chain (β-MHC) and atrial natriuretic peptide (ANP) in cells treated as in **e**. $n = 3$. $^{**}P < 0.01$ vs. NC; $^{\#\#}P < 0.01$ vs. Ang II. Data are presented as the means ± SEM.

the reduction in GJA1-20k expression and development of hypertrophy in the NRCMs stimulated by Ang II.

Levels of mitochondrial GJA1-20k expression are downregulated in the SHRs, and valsartan attenuates this change

Impairment of energy metabolism in CH has been found to occur in close proximity to mitochondria and is one of the main pathogenic mechanisms of CH. Considering the reported localization of GJA1-20k to mitochondria in noncardiac cells and I/R hearts [23, 24], we next explored the level of mitochondrial GJA1-20k expression in SHR hearts. The subcellular expression of GJA1-20k was evaluated in the SHR hearts using mitochondrial biochemical fractionation (Fig. 8a). Similar to the results shown in Fig. 1, decreased mitochondrial levels of GJA1-20k were observed in the SHRs compared to those in the WKY rats, and valsartan also upregulated mitochondrial GJA1-20k expression. GJA1-20k localization to mitochondria was confirmed using structured illumination super resolution microscopy (N-SIM) to acquire images of mitochondria in the NRCMs transfected with GFP-tagged GJA1-20k and then treated with vehicle or Ang II for 48 h (Fig. 8b). These data suggest a potential role of mitochondrial GJA1-20k in the pathogenesis of CH.

Mitochondrial biogenesis is suppressed in the SHRs, and valsartan upregulates the expression of relevant genes

Given the function and tropism of GJA1-20k in cardiac mitochondria, we examined heart tissue lysates from WKY rats, SHRs, and SHR-Val rats to determine the expression of six proteins associated with mitochondrial biogenesis (Fig. 9a, b). The six proteins were significantly increased in the SHRs, and one of them was peroxisome proliferator-activated receptor-γ coactivator-1α (PGC-1α), which is known to be an intranuclear-generated mitochondrial biogenesis "master regulator". In addition, considering the importance of mitochondrial fusion and fission, which can further contribute to new mitochondrial biogenesis, we assessed the expression level of the active form of fission protein Drp1 and fusion protein Mitofusin1 in the SHRs (Fig. 9c, d). As indicated in Fig. 9, WB confirmed that the increase in p-Drp1 and decrease in Mitofusin1 in the SHRs were reversed by valsartan. These results indicate that downregulation of

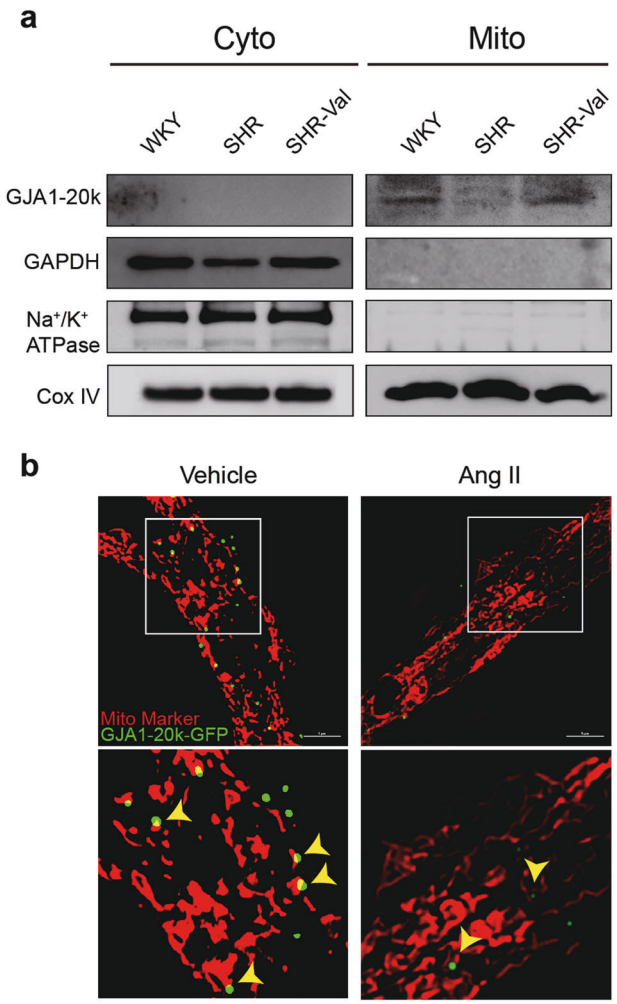

Fig. 8 Mitochondrial GJA1-20k is downregulated in the spontaneously hypertensive rat (SHR) cardiac hypertrophy (CH) model. **a** Biochemical fractionation of hearts from WKY rats, SHRs, and SHR-Val rats. Cox IV is used as a mitochondrial marker. Na^+/K^+ ATPase is used as a plasma membrane marker. Cyto cytosol, Mito mitochondria. **b** N-SIM images of a single cardiomyocyte expressing GFP-tagged GJA1-20k (green). Mitochondrial marker is shown in red (bar = 5 μm).

GJA1-20k may induce the impairment of energy metabolism during the development of CH.

GJA1-20k enhances mitochondrial membrane potential and respiration and lowers ROS production in Ang II-induced cardiomyocyte hypertrophy

Next, to further assess the effect of GJA1-20k on mitochondrial function and cardiac metabolism in CH, we evaluated the mitochondrial membrane potential in Ang II-induced cellular hypertrophic phenotype of the NRCMs by transfecting these cells with an empty vector or GJA1-20k cDNA. JC-1 is a MitoTracker dye that selectively enters mitochondria and reversibly changes from red (active mitochondria) to green (inactive mitochondria) as the membrane potential decreases. Thus, the red/green fluorescence ratio of JC-1 indicates the fraction of active mitochondria at a given time point. As observed in Fig. 10a, b, Ang II increased green fluorescence intensity but decreased red fluorescence intensity, indicating that the mitochondrial membrane potential of the cells was significantly reduced. However, when the cells were transfected with GJA1-20k, before the addition of Ang II, a weak green fluorescence but enhanced red fluorescence were observed, which suggested that GJA1-20k attenuated the collapse of the mitochondrial membrane potential in Ang II-induced CH.

Cardiomyocyte metabolism was also evaluated using Seahorse XF cell Mito Stress assay, which measures the oxygen consumption rate. As shown in Fig. 10c, d, the Seahorse data indicate that the basal respiration, maximal respiration, and nonmitochondrial oxygen consumption were significantly decreased in Ang II-induced CH, and the level of each was enhanced by GJA1-20k.

Finally, mitochondrial metabolic function was assessed in NRCMs with Ang II-induced CH by examining the basal level of mitochondria-generated ROS using confocal microscopy with MitoSOX dye as the fluorescent indicator. MitoSOX red is a fluorogenic dye that specifically targets mitochondria in live cells and is oxidized only in the presence of superoxide agents to fluoresce red. Therefore, the more superoxide agents present in the cell, the higher the fluorescence intensity produced by MitoSOX. The data in Fig. 10e, f indicate that Ang II increased ROS production in NRCMs with Ang II-induced CH, which was reduced after GJA1-20k overexpression. Taken together, our data, as presented in Fig. 10, suggested that GJA1-20k enhances energy metabolism, which may increase ATP production in each mitochondrion. Thus, GJA1-20k can exert cardioprotective effects during the development of CH.

DISCUSSION

In this study, we report for the first time for cardiomyocytes that (1) GJA1-20k is downregulated in CH in both in vitro and in vivo SHR models, (2) valsartan and AG490 attenuate GJA1-20k downregulation and restore the formation of Cx43 GJs during the progression of cardiomyocyte hypertrophy, (3) GJA1-20k downregulation is a key step for cardiomyocyte hypertrophy, (4) Jak2 knockdown in NRCMs attenuates GJA1-20k downregulation and promotes Cx43 gap junction formation in Ang II-induced cell hypertrophy, (5) mitochondrial GJA1-20k is suppressed in the pathogenesis of CH, and (6) overexpression of GJA1-20k enhances energy metabolism in the mitochondria of cells with Ang II-induced cell hypertrophy. GJA1-20k, which promotes Cx43 gap junction formation and regulates mitochondrial function, is a protein that was only very recently discovered to exist because of alternative translation. Understanding the role of GJA1-20k in CH regulation provides specific targets for novel therapies that may prevent the formation of anatomic substrates that cause lethal ventricular arrhythmias in patients with heart disease.

In the mammalian heart, GJs mediate the rapid conduction of electrical impulses that precede coordinated contractions. The normal heart rhythm thus depends fundamentally on the coupling of cardiac myocytes through GJs. Disturbances of normal cardiac rhythm are common, serious, and often fatal complications in many forms of heart diseases, including cardiomyocyte hypertrophy. There is emerging evidence that Cx43, the major gap junction protein expressed in the heart, is extensively remodeled during CH. Usually, Cx43 is downregulated and decreased in the intercalated disks of hypertrophic cardiomyocytes. However, the mechanism of Cx43 gap junction redistribution in CH remains unclear.

GJA1-20k, acting as a chaperone auxiliary protein, has been reported to facilitate the trafficking of GJA1-43k to cell–cell borders. To date, no study has been conducted to investigate whether GJA1-20k influences GJA1-43k localization or gap junction formation in CH. In the present study, we demonstrated that GJA1-20k plays a critical role in Cx43 gap junction formation in Ang II-induced CH. GJA1-20k, the product of the alternative translation of GJA1 mRNA, was recently identified as a novel and key component in Cx43 gap junction formation. Moreover, the expression of a GJA1-20k isoform is predominant in human heart tissue, zebrafish hearts, and many cancer cell lines [22, 32, 33]. Consistent with our results, Basheer et al. [34] reported that

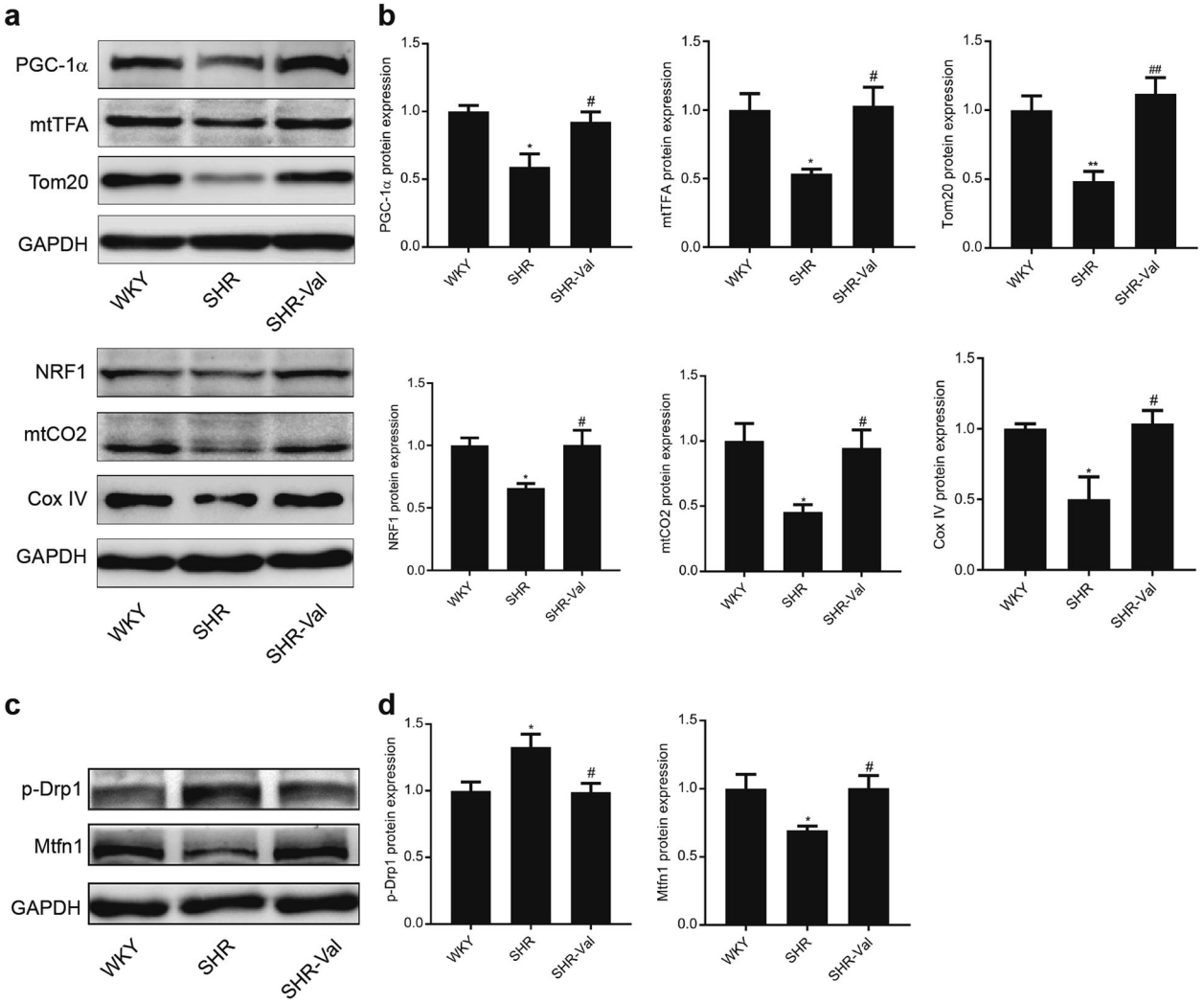

Fig. 9 Mitochondrial biogenesis is suppressed in the spontaneously hypertensive rat (SHR) cardiac hypertrophy (CH) model. a Western blot showing the expression levels of critical transcription factors involved in mitochondrial biogenesis (PGC-1α, mtTFA, and NRF1) and mitochondrial proteins (Tom20, Cox IV, and mtCO2) in the heart lysates from the WKY rats, SHRs, and SHR-Val rats. Quantification of protein expression is shown in **b**. $n = 5–6$. $^{*}P < 0.05$, $^{**}P < 0.01$ vs. WKY; $^{\#}P < 0.05$, $^{\#\#}P < 0.01$ vs. SHR. **c** Western blot showing the amount of active Drp1 fission protein and Mitofusin1 fusion protein in the heart lysates from the WKY, SHR, and SHR-Val groups. Quantification of protein expression is shown in **d**. $n = 5–6$. $^{*}P < 0.05$ vs. WKY; $^{\#}P < 0.05$ SHR. Data are presented as the means ± SEM.

GJA1-20k markedly increased endogenous myocardial Cx43 gap junction plaque size at IDs, which was demonstrated by an in vivo AAV9-mediated gene transfer system. In addition, James et al. [35] demonstrated that the suppression of GJA1-20k expression by TGF-β was sufficient to limit gap junction formation during the EMT. Therefore, we may conclude that decreases in GJs at cell–cell borders, which are caused by a variety of diseases, are attributable to the downregulation of GJA1-20k. However, we cannot exclude the possibility that other mechanisms underlying the redistribution of GJs may also exist. Notably, although GJA1-20k is necessary for the successful trafficking of Cx43 to cell–cell borders, which contributes to gap junction formation, GJA1-20k has no effect on the expression of Cx43.

Previous studies [22, 32] have provided excellent evidence that activation of the mTOR and Mnk1/2 pathways suppresses the expression of GJA1-20k, but we wondered whether GJA1-20k expression is regulated by other signaling pathways associated with translation. Therefore, in this study, we investigated pathways independent of mTOR and Mnk1/2. The pathogenesis of CH was linked to the activation of the RAS pathway, as indicated by the ability of ACE inhibitors and AT1 receptor antagonists, such as valsartan, losartan, and candesartan, to reverse left ventricular hypertrophy (LVH) in patients with hypertension. Several signaling molecules have been implicated in the Ang II-induced hypertrophic response, including JAK and signal transducer and activator of transcription (STAT) [36–39]. Following the chemical inhibition of Jak2 signaling and Jak2 knockdown in the NRCMs, we found a significant increase in the expression of GJA1-20k. Kunisada et al. reported [40] that transgenic mice overexpressing Stat3 in the myocardium showed signs of hypertrophy by 12 weeks of age, their hearts displaying enlarged left ventricles, increased cardiomyocyte width and enhanced expression of the hypertrophic genes β-MHC and ANP. Harada et al. [41] showed that the JAK-STAT pathway has an important role in mediating the effects of G-CSF to prevent left ventricular remodeling after myocardial infarction. Recently, Zeitz et al. [42] reported that, during stress and aging, the activation of stress pathways, such as the P38 and ERK signal transduction pathways, reduced the 5′UTR length of Cx43 mRNA, which was sufficient to inhibit the expression of GJA1-20k, leading to the loss of gap junction formation. Thus, we inferred that the mechanism by which the JAK-STAT pathway reduces GJA1-20k expression is similar. The

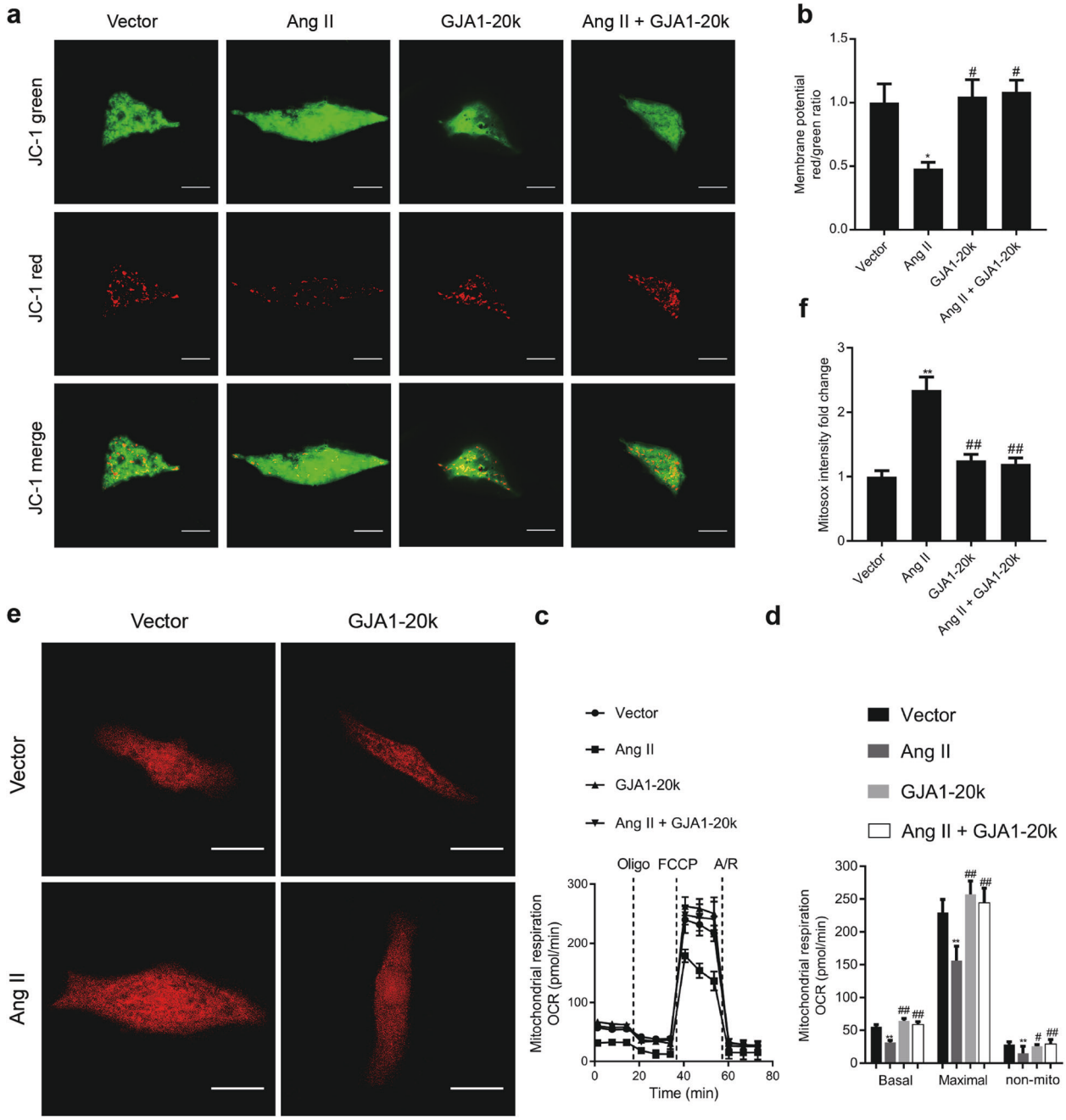

Fig. 10 GJA1-20k enhances energy metabolism in Ang II-induced cardiomyocyte hypertrophy (CH). Twenty-four hours after the empty vector or GJA1-20k cDNA was transfected into neonatal rat cardiomyocytes (NRCMs), the cells were treated with Ang II (1 μM) for 48 h. **a** Mitochondrial membrane potential was determined by JC-1 staining. Red fluorescence represents normal membrane potential, and green fluorescence represents mitochondrial membrane potential depolarization (bar = 20 μm). **b** Ratiometric measurement (red/green) using JC-1 in the four groups. $n = 3$. $^{*}P < 0.05$ vs. vector; $^{\#}P < 0.05$ vs. Ang II. **c** Seahorse XF Cell Mito Stress assay was used for characterization of oxygen consumption (OCR). OCR under basal conditions and in response to the indicated mitochondrial inhibitor is shown over time. **d** Quantification of basal respiration, maximal respiration, and nonmitochondrial respiration in each group is shown with the number of wells assessed per group >10. $n = 3$. $^{**}P < 0.01$ vs. vector; $^{\#}P < 0.05$, $^{\#\#}P < 0.01$ vs. Ang II. **e** Cardiomyocytes were loaded with the fluorogenic dye MitoSOX Red to examine mitochondrial superoxide production; fluorescence intensity as measured and quantified as in **f** reported as a fold change. bar = 20 μm. $n = 3$. $^{**}P < 0.01$ vs. vector; $^{\#\#}P < 0.01$ vs. Ang II. Data are presented as the means ± SEM.

above in vivo studies, together with our present investigation, support our conclusion: In the development of Ang II-induced CH, JAK-STAT is the major mediator of GJA1-20k expression.

Secondary electrical remodeling, which develops as a result of structural insult to the myocardium, is a response to pathological CH. One of the hallmarks of secondary electrical remodeling is repolarization abnormalities, specifically prolonged action potential [43]. Electrical remodeling in the ventricle produces an electrophysiological substrate for the development of potentially malignant ventricular arrhythmia. The mechanisms critical for arrhythmias are complex. Importantly, the remodeling of GJs has been demonstrated in multiple models of secondary electrical remodeling and has been linked to arrhythmia risk [12, 44–46]. The decreased expression and lateralization of Cx43

decreases the conduction velocity and increases the dispersion of repolarization, with both action providing substrates for arrhythmias [47]. Targeted ablation of Cx43 in mice has demonstrated the importance of Cx43 for electrical coupling in various cardiovascular tissues and has shown that its absence can lead to various arrhythmias or sudden death [48, 49]. Therefore, therapies targeting GJs are active areas of investigation. With our results, we demonstrated that GJA1-20k plays a critical role in Cx43 gap junction formation in cardiomyocytes; it attenuated Ang II-induced hypertrophy and decreased cell size and β-MHC and ANP expression by regulating gap junction formation. These findings may contribute to the restoration of key electrophysiological properties of the heart and minimize the occurrence of arrhythmias.

Based on the data from numerous in vitro and in vivo studies, such as those using knockout/knock-in and pharmacologic approaches, it has become clear that Cx43 GJs play important roles in cardiac disease development and prevention. In contrast, when defective, connexins can cause diseases involving hypertrophy, electrophysiological changes, arrhythmia, ischemia-reperfusion injury, and heart failure [50, 51]. Rotigaptide, an antiarrhythmic drug developed by Zealand Pharma, exerts antiarrhythmic effects by increasing communication and conduction through Cx43-mediated GJs in cell cultures and in a variety of animal models [52–55]. Moreover, on the basis of rotigaptide results, Zealand developed the next-generation gap junction modifier, danegaptide [56, 57]. Several studies confirmed that danegaptide reduced infarct size following ischemia-reperfusion injury (IRI) in pigs; further, it decreased cardiomyocyte hypercontracture and exhibited antiarrhythmia effects on fibrillation in dogs [58, 59]. Basheer et al. provided further evidence [34] that GJA1-20k protects Cx43 localization at IDs upon acute ischemic injury using an in vivo AAV9-mediated gene delivery system, which indicated that GJA1-20k is a potential therapeutic target to prevent ischemic cardiac injury. However, their study provided little evidence about the effect of GJA1-20k on acute ischemic injury. Moreover, in an investigation by James et al., the expression of GJA1-20k was sufficient to rescue gap junction formation, but it did not halt EMT processes [35]. The difference in the GJA1-20k effect on various diseases may be the result of gap junction coupling itself. A number of factors influence gap junction coupling, including the amount and types of connexin expressed, the size and distribution of gap junction plaques, the proportion of each connexin assembled into functional junctions, and the gating and specific connexin of individual gap junction channels. Together, these results indicate that further experiments are needed to study the effect and function of GJA1-20k.

In addition to promoting Cx43 gap junction formation, GJA1-20k shows strong tropism for mitochondria in noncardiac and I/R hearts. Fu [23] found that GJA1-20k appears to be an organelle chaperone and that overexpression of GJA1-20k is sufficient to rescue mitochondrial localization to the cell periphery upon exposure to hydrogen peroxide. Moreover, Wassim A. Basheer found [24] that GJA1-20k is an endogenous stress response protein that induces mitochondrial biogenesis and metabolic hibernation, preconditioning the heart against I/R insults. However, in our present experiments, we found that GJA1-20k enhanced mitochondrial membrane potential and respiration and lowered ROS production in Ang II-induced cardiomyocyte hypertrophy, resulting in the production of ATP in mitochondria. The reason for the differences in the effects of GJA1-20k on various diseases remains unclear. Thus, more experiments are needed to study the effect and function of GJA1-20k.

There are several limitations to our study. (1) Because our experiments were mainly performed in cultured cardiomyocytes, GJA1-20k-mediated gap junction formation and its effect on CH need to be further verified in SHR models by using an in vivo adeno-associated virus serotype 9 (AAV9)–mediated gene transfer system. (2) Further molecular and cellular studies are needed to address the mechanism by which activated Jak2 downregulates GJA1-20k and CH. (3) Finally, our conclusions may be applicable only to cardiomyocyte hypertrophy.

In summary, our results revealed that GJA1-20k plays a key role in CH by regulating Cx43 gap junction formation, enhancing energy metabolism, reducing cell size, and attenuating cardiomyocyte hypertrophy, and the mechanism involves the suppression of the JAK-STAT signaling pathway. Therefore, our results reveal a mechanism of Ang II signaling in cardiomyocytes that is mediated through JAK2/STAT3. Ang II induces CH through Jak2-mediated downregulation of GJA1-20k, which is associated with gap junction coupling and mitochondrial function. Overall, our study identifies a novel pathway, Ang II → JAK2/STAT3 → GJA1-20k → gap junction formation or mitochondrial function, which plays a pathophysiological role in the development of CH. Further studies are needed to address the question of whether the effect of GJA1-20k on CHy is similar in vivo.

ACKNOWLEDGEMENTS

This work was supported by the National Natural Science Foundation of China (grant No. 81473234), the Joint Fund of the National Natural Science Foundation of China (grant No. U1303221), the Guangdong Basic and Applied Basic Research Foundation (grant No. 2019A1515012215), and a grant from the Department of Science and Technology of Guangdong Province (grant No. 20160908).

AUTHOR CONTRIBUTIONS

LT and QW conceived and designed the study. YLF and FHP performed the siRNA and cDNA transfection experiments, qPCR and Western blot analyses. NZZ and QL performed the flow cytometry experiments and immunofluorescence and collected and analyzed the data. SYC was involved in cell culture and made substantial contributions to the acquisition and interpretation of the data. YLF wrote the manuscript. LT and QW revised and amended the draft. QW contributed to the final approval of the version to be published. All authors read and approved the final manuscript and agree to be accountable for all aspects of the research in ensuring that the accuracy and integrity of all parts of the work are appropriately investigated and resolved.

ADDITIONAL INFORMATION

The online version of this article (https://doi.org/10.1038/s41401-020-0459-6) contains supplementary material, which is available to authorized users.

Competing interests: The authors declare no competing interests.

REFERENCES

1. Frey N, Olson EN. Cardiac hypertrophy: the good, the bad, and the ugly. Annu Rev Physiol. 2003;65:45–79.
2. Heineke J, Molkentin JD. Regulation of cardiac hypertrophy by intracellular signalling pathways. Nat Rev Mol Cell Biol. 2006;7:589–600.
3. Lips DJ, dewindt LJ, Van Kraaij DJ, Doevendans PA. Molecular determinants of myocardial hypertrophy and failure: alternative pathways for beneficial and maladaptive hypertrophy. Eur Heart J. 2003;24:883–96.
4. Ritter O, Neyses L. The molecular basis of myocardial hypertrophy and heart failure. Trends Mol Med. 2003;9:313–21.
5. Chien KR, Knowlton KU. Regulation of cardiac gene expression during myocardial growth and hypertrophy: molecular studies of an adaptive physiologic response. FASEB J 1991;5:3037–46.
6. Bruzzone HarrisAL, Locke D. Connexins: a guide. Mol Biotechnol 2009;43:12300–9.
7. Saffitz JE, Hames KY, Kanno S. Remodeling of gap junctions in ischemic and nonischemic forms of heart disease. J Membr Biol. 2007;218:65–71.
8. Severs NJ, Bruce AF, Dupont E, Rothery S. Remodelling of gap junctions and connexin expression in diseased myocardium. Cardiovasc Res 2008;80:9–19.
9. Peters NS. New insights into myocardial arrhythmogenesis: distribution of gap-junctional coupling in normal, ischaemic and hypertrophied hearts. Clin Sci. 1996;90:447–52.
10. Kostin S, Rieger M, Dammer S, Hein S, Richter M, Klövekorn WP, et al. Gap junction remodeling and altered connexin43 expression in the failing human heart. Mol Cell Biochem. 2003;242:135–44.

11. Kitamura H, Ohnishi Y, Yoshida A, Okajima K, Azumi H, Ishida A, et al. Heterogeneous loss of connexin43 protein in nonischemic dilated cardiomyopathy with ventricular tachycardia. J Cardiovasc Electrophysiol. 2002;13:865–70.
12. Dupont E, Matsushita T, Kaba RA, Vozzi C, Coppen SR, Khan N, et al. Altered connexin expression in human congestive heart failure. J Mol Cell Cardiol. 2001;33:359–71.
13. Angeliki A, Sudhir K, Eva P, Anne KA, Edward A, Zhenzhen L, et al. Identification of a new modulator of the intercalated disc in a zebrafish model of arrhythmogenic cardiomyopathy. Sci Transl Med. 2014;6:240–74.
14. Remo BF, Giovannone S, Fishman GI. Connexin43 cardiac gap junction remodeling: lessons from genetically engineered murine models. J Membr Biol. 2012;245:275–81.
15. Spach MS, Boineau JP. Microfibrosis produces electrical load variations due to loss of side-to-side cell connections: a major mechanism of structural heart disease arrhythmias. Pacing Clin Electrophysiol. 1997;20:397–413.
16. Zhou LY, Liu JP, Wang K, Gao J, Ding SL, Jiao JQ, et al. Mitochondrial function in cardiac hypertrophy. Int J Cardiol. 2013;167:1118–25.
17. Wikman-Coffelt J, Parmley WW, Mason DT. The cardiac hypertrophy process. Analyses of factors determining pathological vs. physiological development. Circ Res. 1979;45:697–707.
18. Vinken M, Decrock E, Leybaert L, Bultynck G, Himpens B, Vanhaecke T, et al. Non-channel functions of connexins in cell growth and cell death. Biochim Biophys Acta. 2012;1818:2002–8.
19. Kardami E, Dang X, Iacobas DA, Nickel BE, Jeyaraman M, Srisakuldee W, et al. The role of connexins in controlling cell growth and gene expression. Prog Biophys Mol Biol. 2007;94:245–64.
20. Jiang JX, Penuela S. Connexin and pannexin channels in cancer. BMC Mol Cell Biol. 2016;17:12–26.
21. Aasen T, Mesnil M, Naus CC, Lampe PD, Laird DW. Gap junctions and cancer: communicating for 50 years. Nat Rev Cancer. 2016;16:775–88.
22. Smyth JW, Shaw RM. Autoregulation of connexin43 gap junction formation by internally translated isoforms. Cell Rep. 2013;5:611–8.
23. Fu Y, Zhang SS, Xiao S, Basheer A, Baum R, Epifantseva I, et al. Cx43 isoform GJA11-20k promotes microtubule dependent mitochondrial transport. Front Physiol 2017;8:905–17.
24. Basheer WA, Fu Y, Shimura D, Xiao S, Agvanian S, Hernandez DM, et al. Stress response protein GJA1-20k promotes mitochondrial biogenesis, metabolic quiescence, and cardioprotection against ischemia/reperfusion injury. JCI Insight 2018;3:378–90.
25. Yang D, Xi J, Xing Y, Tang X, Dai X, Li K, et al. A new method for neonatal rat ventricular myocyte purification using superparamagnetic iron oxide particles. Int J Cardiol. 2018;270:293–301.
26. Wang Y, Wang F, Yang D. Berberine in combination with yohimbine attenuates sepsis-induced neutrophil tissue infiltration and multiorgan dysfunction partly via IL-10-mediated inhibition of CCR2 expression in neutrophils. Int Immunopharmacol. 2016;35:217–25.
27. Xiang Y, Wang Q, Guo Y, Ge H, Fu Y, Wang X, et al. Cx32 exerts anti-apoptotic and pro-tumor effects via the epidermal growth factor receptor pathway in hepatocellular carcinoma. J Exp Clin Cancer Res. 2019;38:145–60.
28. Doser TA, Turdi S, Thomas DP, Epstein PN, Li SY, Ren J. Transgenic overexpression of aldehyde dehydrogenase-2 rescues chronic alcohol intake-induced myocardial hypertrophy and contractile dysfunction. Circulation 2009;119:1941–9.
29. Shi Z, Wei Z, Li J, Yuan S, Pan B, Cao F, et al. Identification and verification of candidate genes regulating neural stem cells behavior under hypoxia. Cell Physiol Biochem. 2018;47:212–22.
30. Subramanian A, Tamayo P, Mootha VK, Mukherjee S, Ebert BL, Gillette MA, et al. Gene set enrichment analysis: a knowledge-based approach for interpreting genome-wide expression profiles. Proc Natl Acad Sci USA. 2005;102:15545–50.
31. Shah BH, Catt KJ. A central role of EGF receptor transactivation in angiotensin II-induced cardiac hypertrophy. Trends Pharmacol Sci. 2003;24:239–44.
32. Salat-Canela C, Sesé M, Peula C, Cajal SRY, Aasen T. Internal translation of the connexin 43 transcript. Cell Commun Signal. 2014;12:31–44.
33. Chatterjee B, Chin AJ, Valdimarsson G, Finis C, Sonntag JM, Choi BY, et al. Developmental regulation and expression of the zebrafish connexin43 gene. Dev Dynam. 2005;233:890–906.
34. Basheer WA, Xiao S, Epifantseva I, Fu Y, Kleber AG, Hong T, et al. GIA1-20k arranges actin to guide Cx43 delivery to cardiac intercalated discs. Circ Res 2017;121:1069–80.
35. James CC, Zeitz MJ, Calhoun PJ, Lamouille S, Smyth JW. Altered translation initiation of GJA1 limits gap junction formation during epithelial–mesenchymal transition. Mol Biol Cell. 2018;29:797–808.
36. Booz GW, Day JN, Baker KM. Interplay between the cardiac renin angiotensin system and JAK-STAT signaling: role in cardiac hypertrophy, ischemia/reperfusion dysfunction, and heart failure. J Mol Cell Cardiol. 2002;34:1443–53.
37. Mascareno E, Dhar M, Siddiqui MA. Signal transduction and activator of transcription (STAT) protein-dependent activation of angiotensinogen promoter: a cellular signal for hypertrophy in cardiac muscle. Proc Natl Acad Sci USA. 1998;95:5590–4.
38. Mascareno E, Siddiqui MA. The role of Jak/STAT signaling in heart tissue renin–angiotensin system. Mol Cell Biochem. 2000;212:171–5.
39. Rohini A, Agrawal N, Koyani CN, Singh R. Molecular targets and regulators of cardiac hypertrophy. Pharmacol Res. 2010;61:269–80.
40. Kunisada K, Negoro S, Tone E, Funamoto M, Osugi T, Yamada S, et al. Signal transducer and activator of transcription 3 in the heart transduces not only a hypertrophic signal but a protective signal against doxorubicin-induced cardiomyopathy. Proc Natl Acad Sci USA. 2000;97:315–9.
41. Harada M, Qin Y, Takano H, Minamino T, Zou Y, Toko H, et al. G-CSF prevents cardiac remodeling after myocardial infarction by activating the Jak-Stat pathway in cardiomyocytes. Nat Med 2005;11:305–11.
42. Zeitz MJ, Calhoun PJ, James CC, Taetzsch T, George KK, Robel S, et al. Dynamic UTR usage regulates alternative translation to modulate gap junction formation during stress and aging. Cell Rep. 2019;27:2737–47.
43. Cutler MJ, Jeyaraj D, Rosenbaum DS. Cardiac electrical remodeling in health and disease. Trends Pharmacol Sci. 2011;32:174–80.
44. Pozlzing S, Rosenbaum DS. Altered Connexin43 expression produces arrhythmia substrate in heart failure. Am J Physiol Heart Circ Physiol. 2004;287:1762–70.
45. Akar FG, Nass RD, Hahn S, Tomaselli GF. Dynamic changes in conduction velocity and gap junction properties during development of pacing-induced heart failure. Am J Physiol Heart Circ Physiol. 2007;293:1223–30.
46. Akar FG, Spragg DD, Tunin RS, Kass DA, Tomaselli GF. Mechanisms underlying conduction slowing and arrhythmogenesis in nonischemic dilated cardiomyopathy. Circ Res. 2004;95:717–25.
47. Danik SB, Liu F, Zhang J. Modulation of cardiac gap junction expression and arrhythmic susceptibility. Circ Res. 2004;95:1035–41.
48. Gutstein DE, Morley GE, Tamaddon H, Vaidya D, Schneider MD, Chen J, et al. Conduction slowing and sudden arrhythmic death in mice with cardiac-restricted inactivation of connexin43. Circ Res. 2001;88:333–9.
49. Gutstein DE, Morley GE, Vaidya D, Fishman GI. Heterogeneous expression of gap junction channels in the heart leads to conduction defects and ventricular dysfunction. Circulation. 2001;104:1194–9.
50. Leybaert L, Lampe PD, Dhein S, Kwak BR, Ferdinandy P, Beyer EC, et al. Connexins in cardiovascular and neurovascular health and disease: pharmacological implications. Pharmacol Rev. 2017;69:396–478.
51. Hesketh GG, Shah MH, Halperin VL, Cooke CA, Akar FG, et al. Ultrastructure and regulation of lateralized connexin43 in the failing heart. Circ Res. 2010;106:1153–63.
52. Dhein S, Manicone N, Müller A, Gerwin R, Ziskoven U, Irankhahi A, et al. A new synthetic antiarrhythmic peptide reduces dispersion of epicardial activation recovery interval and diminishes alterations of epicardial activation patterns induced by regional ischemia. Naunyn Schmiedebergs Arch Pharmacol. 1994;350:174–84.
53. Lin X, Zemlin C, Hennan JK, Petersen JS, Veenstra RD. Enhancement of ventricular gap-junction coupling by rotigaptide. Cardiovasc Res. 2008;79:416–26.
54. Clarke TC, Thomas D, Petersen JS, Evans WH, Martin PE. The antiarrhythmic peptide rotigaptide (ZP123) increases gap junction intercellular communication in cardiac myocytes and HeLa cells expressing connexin43. Br J Pharmacol. 2006;147:486–95.
55. Jorgensen NR, Teilmann SC, Henriksen Z, Meier E, Hansen SS, Jensen JE, et al. The antiarrhythmic peptide analog rotigaptide (ZP123) stimulates gap junction intercellular communication in human osteoblasts and prevents decrease in femoral trabecular bone strength in ovariectomized rats. Endocrinology. 2005;146:4745–54.
56. Rossman EI, Liu K, Morgan GA, Swillo RE, Krueger JA, Gardell SJ, et al. The gap junction modifier, improves conduction and reduces atrial fibrillation/flutter in the canine sterile pericarditis model. J Pharmacol Exp Ther. 2009;329:1127–33.
57. Laurent G, Leong-Poi H, Mangat I, Moe GW, Hu X, So PP, et al. Effects of chronic gap junction conduction-enhancing antiarrhythmic peptide GAP-134 administration on experimental atrial fibrillation in dogs. Circ Arrhythmia Electrophysiol. 2009;2:171–8.
58. Boengler K, Bulic M, Schreckenberg R, Schlüter KD, Schulz R. The gap junction modifier ZP1609 decreases cardiomyocyte hypercontracture following ischaemia/reperfusion independent from mitochondrial connexin43. Br J Pharmacol. 2017;174:2060–73.
59. Skyschally A, Walter B, Schultz Hansen R, Heusch G. The antiarrhythmic dipeptide ZP1609 (danegaptide) when given at reperfusion reduces myocardial infarct size in pigs. Naunyn Schmiedebergs Arch Pharmacol. 2013;386:383–91.